Biochemical and Biophysical Research Communications 472 (2016) 566–571

Contents lists available at ScienceDirect

Biochemical and Biophysical Research Communications

journal homepage: www.elsevier.com/locate/ybbrc

Coiled-coil forming peptides for the induction of silver nanoparticles

Sabina Božič Abram [a, b], Jana Aupič [a, c], Goran Dražić [d], Helena Gradišar [a, e], Roman Jerala [a, e, *]

[a] Department of Synthetic Biology and Immunology, National Institute of Chemistry, Hajdrihova 19, 1000 Ljubljana, Slovenia
[b] Graduate School of Biomedicine, University of Ljubljana, Ljubljana 1000, Slovenia
[c] Doctoral Programme in Chemical Sciences, Faculty of Chemistry and Chemical Technology, University of Ljubljana, Ljubljana 1000, Slovenia
[d] Laboratory for Materials Chemistry, National Institute of Chemistry, Hajdrihova 19, 1000 Ljubljana, Slovenia
[e] EN-FIST, Centre of Excellence, Trg Osvobodilne fronte 13, Ljubljana 1000, Slovenia

ARTICLE INFO

Article history:
Received 7 March 2016
Accepted 9 March 2016
Available online 10 March 2016

Keywords:
Silver nanoparticles
Antibacterial activity
Coiled-coils
Plasmon resonance
QSAR analysis

ABSTRACT

Biopolymers with defined sequence patterns offer an attractive alternative for the formation of silver nanoparticle (AgNP). A set of coiled-coil dimer forming peptides was tested for their AgNP formation ability. Seventeen of those peptides mediated the formation of AgNPs in aqueous solution at neutral pH, while the formation of a coiled-coil dimer inhibited the nanoparticle generation. A QSAR regression model on the relationship between sequence and function suggests that in this peptide type the patterns KXQQ and KXEE are favorable, whereas Ala residues appear to have an inhibitory effect. UV–VIS spectra of the obtained nanoparticles gave a peak at around 420 nm, typical for AgNPs in the size range around 40 nm, which was confirmed by dynamic light scattering and transmission electron microscopy. Peptide-induced AgNPs exhibited good antibacterial activity, even after a 15 min contact time, while they had low toxicity to human cells at the same concentrations. These results show that our designed peptides generate AgNPs with antibacterial activity at mild conditions and might be used for antibacterial coatings.

1. Introduction

Silver nanoparticles (AgNP) have already achieved a widespread use, primarily due to their antimicrobial activity. Besides chemical formation an alternative method for their production is the use of molecules that induce generation of homogeneous size nanoparticles, such as peptides with a specified sequence [1–4]. The advantage of peptides as AgNP inducing molecules is that peptides may be attached to the selected surfaces or fused to other functional proteins, such as antibodies, enabling production of smart materials.

In the recent years coiled-coils proved to be one of the most promising designed protein nanostructure building modules [5–7]. This protein structural motif is characterized by a specific seven amino acid repeat denoted *abcdefg* (heptad). The rules by which structure, oligomerization and partner specificity occur are very well understood and relatively straightforward; specific di(oligo) merization is guided by hydrophobic interactions between amino acid residues at positions *a* and *d* and electrostatic interactions between positions *e* and *g* of the heptad repeat. This knowledge has been exploited in the past for *de novo* design of coiled-coil peptides to generate sets of interacting peptides [8–10]. Much effort has been put into the design of a molecular toolbox for protein nanostructure design [11]. One of the advantages of a protein based platform, compared to the DNA nanostructures, is the chemical diversity of amino acid functional groups. Several interesting functionalities have been explored in the context of coiled-coils, such as triggered oligomerization, conformational change [12] or quantum dot binding [13,14].

Recently a great deal of effort has been put into investigating peptides for their silver nanoparticle formation abilities. This is mainly due to the fact that formation of metal nanoparticles via peptides occurs in an aqueous environment, at room temperature without the need for toxic chemicals in contrast to the conventional AgNP production methods. One of the great potentials of silver nanoparticles is their broad antimicrobial activity [15–17]. Despite importance of silver nanoparticle formation, to our knowledge, coiled-coil forming peptides have not been tested for the growth of

* Corresponding author. Department of Synthetic Biology and Immunology, National Institute of Chemistry, Hajdrihova 19, 1000 Ljubljana, Slovenia.
E-mail address: roman.jerala@ki.si (R. Jerala).

http://dx.doi.org/10.1016/j.bbrc.2016.03.042
0006-291X/

metal nanoparticles. This comes somewhat as a surprise given the vast number of such peptides available. Silver coordinating residues, tyrosine and tryptophan, which have been shown to reduce silver ions [18,19], could be introduced into coiled-coil forming peptides at positions *b*, *c* and *f* without interfering with oligomerization, specificity or stability. Previous silver binding and AgNP forming peptides were found via the phage display method in which a large number of randomly generated peptides were expressed at the surface of bacteriophages and selected for their silver affinity [20]. Here we demonstrate results of the analysis of the set of peptides designed for their coiled-coil dimer forming propensities which were tested for silver nanoparticle formation ability and antimicrobial activity of the resulting nanoparticles. This study provides clues to the residues and sequence motifs important for AgNP formation.

2. Materials and methods

2.1. Nanoparticle formation

For the preparation of nanoparticles, synthetic peptides in aqueous solution were used (purchased from China peptides and Genscript) at a concentration of 0.2 mg/ml. $AgNO_3$ was added to peptides to a final concentration of 100 mM. Solutions were held overnight at room temperature and ambient fluorescent light. The solutions were then dialyzed against 5 mM sodium citrate for stabilization of nanoparticles and remaining $AgNO_3$ removal.

2.2. Nanoparticle characterization

UV–VIS spectrometry was performed on Agilent Carry 8454 UV–VIS spectrophotometer. Absorbance was measured in the range from 200 nm to 800 nm. Molar concentrations of silver nanoparticles were calculated using extinction coefficients from the literature ($\varepsilon = 537 \times 10^8\ M^{-1}\ cm^{-1}$ [21]) and are shown in Table 1. Mass concentrations of peptide generated AgNP were estimated from UV–VIS spectra in comparison with commercially available 40 nm silver nanoparticles (purchased from SIGMA ALDRICH cat. no. 730807-25 ML). Particle size was determined by dynamic light scattering (DLS) obtained with Malvern Zetasizer DLS (Malvern, UK) at 20 °C using an angle of 173° and 633 nm laser. For transmission electron microscopy (TEM) 5 μl of silver nanoparticle suspension was put on a copper carbon coated Holey grid and left to dry. Visualization and elemental analysis was performed on Jeol ARM 200 CF probe Cs corrected TEM/STEM, equipped with Centurio 100 mm^2 energy-dispersive X-ray spectrometer (EDXS), at 120 kV accelerating voltage and 50.000x magnification.

Table 1
Absorbance at 420 nm of peptide induced nanoparticles with respective AgNP molar concentrations.

Peptides	Sequence	$A_{420\ nm}$	c (pmol/L)
P4C2	KIEELKQKIEQLKQENQQLEEENSQLEYGC	0.2478	4.615
P5SC23	ENQSLESKISQLKRKNEELKQEISQLEYGC	0.2201	4.099
P4C1	KISQLKQKIQQLKQENQRLEEENRRLEYGC	0.211	3.93
P3sneg8B	DEIEKLEREIEKLEEKNEELKEKNEELKYG	0.1877	3.496
P6SC2R	KNERLKEEIQRLEQENQQLEEKIQRLKYGC	0.1844	3.434
P3SM	EIQQLEEEISQLEQKNSQLKEKNQQLKYG	0.1831	3.41
P4SNEG8	DKIEELKQKIEELKQENEELEEENEELEYG	0.1408	2.621
P3C1	EIQQLEEEISQLEYKNYALKAKNEELKRGC	0.1226	2.283
P5SN	ENSQLEEKISQLKQKNSELKEEIQQLEYG	0.1205	2.245
P6SCW1	KNSQLKEEIQQLEEENQSLEQKIQQLKYGC	0.1027	1.912
P3C2	EIQQLEEEIRQLEQKNSQLKEKNQQLKYGC	0.08	1.49
P6SC23	KNSQLKQEIQSLEEENRRLESKISQLKYGC	0.0783	1.457
P8SM	KISQLKEENQQLEQKIQQLKEENSQLEYG	0.0724	1.349
P5SCW1	ENSQLEEKISQLKQKNSQLKQEIRRLEYGC	0.0723	1.347
P4SM	KISQLKQKIQQLKQENQQLEEENSQLEYG	0.0586	1.091
P3CP	EIQRLEQEIQRLEQKNRRLKQKNRRLKYG	0.0554	1.031
P7SM	EIQSLEEKNSQLKQEISQLEEKNQQLKYG	0.0526	0.98
P3SNEG8	DEIEELEEEIEELEQKNEELKEKNEELKYG	0.0479	0.891
P6SN	KNSELKEEIQQLEEENQQLEEKISELKYG	0.0433	0.806
P5SC2	ENARLEEKIRQLKQKNSQLKEEIQQLEYGC	0.0323	0.601
P5SM	ENAALEQKIAQLKQKNAALKQEIQALEYG	0.0316	0.588
P4CP	KIRRLKEKIRRLKQENRRLEQENRRLEYG	0.0308	0.573
P5SC1	ENSQLEEKISQLKQKNSRLKEEIARLEYGC	0.0291	0.542
P6SC2	KNERLKEEIQRLEQENQQLEEKISQLKYGC	0.0255	0.475
P6SC1	KNSQLKEEIQQLEEENQQLEEKIRQLKYGC	0.0243	0.452
P3	SPEDEIQQLEEEIAQLEQKNAALKEKNQALKYG	0.0148	0.275
P4	SPEDKIAQLKQKIQALKQENQQLEEENAALEYG	0.0084	0.156
P7	SPEDEIQALEEKNAQLKQEIAALEEKNQALKYG	0.0031	0.057
P2	SPEDKIAQLKEKNAALKEKNQQLKEKIQALKYG	0.0029	0.053
P8	SPEDKIAQLKEENQQLEQKIQALKEENAALEYG	0.0008	0.014

2.3. Antibacterial activity

Antimicrobial activity was evaluated against *Escherichia coli* ATCC 11775. The cells were grown overnight at 37 °C and 160 rpm in LB (Luria–Bertani medium). Afterwards they were inoculated at $OD_{600} = 0.1$ and grown to reach the exponential growth phase at approximately $OD_{600} = 0.8$. Bacteria were subsequently diluted to $OD_{600} = 0.01$ and incubated with 2 μg/ml peptide-generated nanoparticles for 1 h at room temperature with shaking at 700 rpm. Concentration dependence of antimicrobial activity was evaluated by varying the concentrations of peptide generated silver nanoparticles. 2 μg/ml, 1 μg/ml, 0.5 μg/ml, 0.25 μg/ml or 0.125 μg/ml of AgNP solutions were added to the same amount of cells and incubated with shaking for 1 h. The effect of the contact duration was tested by plating cells after 15 min, 30 min, 1 h or 2 h incubation with peptide induced AgNPs. In all experiments aqueous solution of 5 mM sodium citrate was used as a control.

2.4. Mammalian cell viability test

Silver nanoparticles were tested for their cytotoxicity against mammalian cells. HEK293T cells were seeded in 96-well plates and exposed to different concentrations of peptide-induced AgNP overnight in triplicates. Cell proliferation was determined by XTT (sodium 3-[1-(phenylaminocarbonyl)-3,4-tetrazolium]-bis(4-methoxy-6-nitro) benzene sulfonic acid hydrate)) assay as described in literature [22]. Cells without nanoparticles were used as negative control and cells that were exposed overnight to 0.001% Triton-X 100 as positive control. Cells were cultured in DMEM (Dulbecco/Vogt modified Eagle's minimal essential medium) medium with 10% FBS (Gibco, Invivogen) at 5% CO_2 and 37 °C.

2.5. QSAR model

In order to identify the underlying sequence motifs of inspected peptides facilitating production of silver nanoparticles a QSAR analysis was performed using experimentally determined absorbance values at 420 nm and a set of descriptors based solely on the peptide sequence. For the calculation of physicochemical descriptors in-house PEDES (peptide descriptors from sequence) computer software was used [23]. Reduction capabilities of peptides were modeled as a linear combination of selected descriptors:

$$log(A_{420nm}(j)) = \sum_{i=1}^{N} a_i P_i(j) + C,$$

where N is the number of descriptors, $P_i(j)$ is the value of the *i*-th descriptor for peptide *j* and a_i are model coefficients.

3. Results and discussion

3.1. Nanoparticle formation and characterization

Recently a highly orthogonal coiled-coil peptide set has been designed, characterized [8] and implemented to design a new protein fold from a single polypeptide chain [24]. In order to alter solubility, helical propensity and effect on the coiled-coil dimer stability, a set of peptides was designed and tested (Table 1). One of the features of these peptides is their high content of negatively charged amino acid residues that coordinate silver or other cations and the presence of a tyrosine residue at the C-terminus, which has been proposed to be involved in silver reduction. We anticipated that these peptides may not only be able to form coiled-coils but might also mediate the reduction of silver ions. Silver nanoparticles have a characteristic plasmon resonance peak at wavelengths from 400 nm to 500 nm, depending on the size of nanoparticles. With increasing particle size, plasmon resonance peak shifts towards longer wavelengths. We took advantage of this feature to test nanoparticle formation ability of each of the 30 peptides in the set. Peptides at a concentration of 0.2 mg/ml were mixed with $AgNO_3$. Interestingly, after 12 h of incubation at room temperature and ambient light we were able to observe a distinct yellow to orange coloration of solution for 17 of the 30 peptides tested (Table 1). The resulting concentrations of nanoparticles were from 1 to 4 pM, as calculated from the measured A_{420}. The majority of peptides gave a typical plasmon resonance peak with a maximum at around 420 nm, one that corresponds to particles in the size range of around 40 nm (Fig. 1a). The control without peptides remained colorless, and no plasmon resonance peak was observed. We decided to inspect two of the peptides with the highest plasmon resonance peaks more thoroughly. We chose peptides P4C2, and P5SC23. The size distribution of silver nanoparticles formed by these peptides was measured by dynamic light scattering, and it proved to be into accordance with the UV–VIS spectra, with the majority of particles around 40 nm for P4C2 and around 30 nm for P5SC23 (Fig. 1b).

Further on we analyzed the samples by transmission electron microscopy. We observed homogeneous particles with sizes similar to those measured by DLS (Fig. 2a). To prove the nanoparticles were indeed AgNPs, we performed EDXS analysis, which showed a clear peak typical for silver (Fig. 2b). We were intrigued by the fact that only some of the tested peptides were capable of AgNP formation. Since the rules governing coiled-coil oligomerization are straightforward and primarily involve four of the seven positions of a coiled-coil heptad repeat, the sequence motifs of the peptides used in this study are quite similar; nevertheless, their abilities to form silver nanoparticles differed significantly despite their sequence similarity. The selected peptides were designed to form heterodimers, therefore none of the peptides was helical in the absence of its corresponding dimerization partner. After formation of AgNPs peptides were still able to form α-helical coiled-coil dimers, while mixing the appropriate pair of coiled-coil dimer forming peptides prior to $AgNO_3$ addition suppressed the occurrence of the plasmon resonance peak, allowing modulation of AgNP formation by the amount of the peptide pairs. This suggests either that the residues involved in dimerization are also involved in the AgNP formation or that the helical conformation is not favorable for the formation of AgNP. The latter explanation is more likely, since the residues involved in coiled-coil dimer formation are conserved in the peptides that had significantly different AgNP formation propensity (e.g. peptide P4 and peptide P4C2, Table 1). The large difference in AgNP formation upon addition of a pairing peptide represents a potentially useful tool for the regulation of AgNP formation in isolated peptides as well as those fused to a larger protein.

Additionally we can conclude that Tyr residues, which have been implicated in silver ion reduction, are not sufficient for the AgNP formation, since they are present in all investigated peptides. Neither is sufficient the mere presence of charged amino acids, such as Glu or Lys, which are quite frequent in the tested peptide set. In order to shed light to the characteristics that are important for AgNP formation in this set of coiled-coil forming peptides, we turned to a quantitative structure–activity relationship (QSAR) model, to extract the relationship between sequence and nanoparticle formation.

3.2. QSAR analysis

We began the QSAR analysis by calculating a wide range of peptide descriptors encompassing sequence dependent physicochemical properties and amino acid composition. In the latter case the frequency of the occurrence of single amino acids was examined, along with the specific clusters of amino acids that have been previously suggested to promote the reduction of silver ions [3,25] as well as amino acid motifs of different lengths. The initial set of descriptors was shrunk to avoid over-fitting. For the selection of the final set of descriptors we used a partial least-squares (PLS) regression. Descriptors included in the model were those that showed to be the most correlated with observed absorbance from the PLS loading plots. The most prominent identified descriptors were the number of occurrence of two sequential glutamic acids in the peptide sequence, number of times the motif with Lys one amino acid removed from two sequential Gln or Glu residues (KXQQ, KXEE as well as QQXK, EEXK motif) appears in the

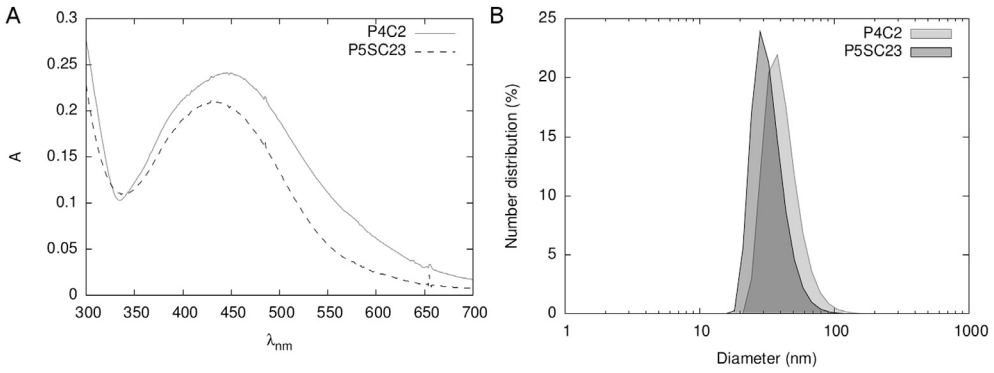

Fig. 1. Characterization of peptide-generated AgNP (**A**) UV–Vis spectra of silver nanoparticles induced by peptides P4C2 and P5SC23 with a maximum at 420 nm (**B**) The hydrodynamic radius of C the peptide-induced AgNP was 40 nm ± 15 nm and 30 nm ± 10 nm for peptides P4C2 and P5SC23, respectively.

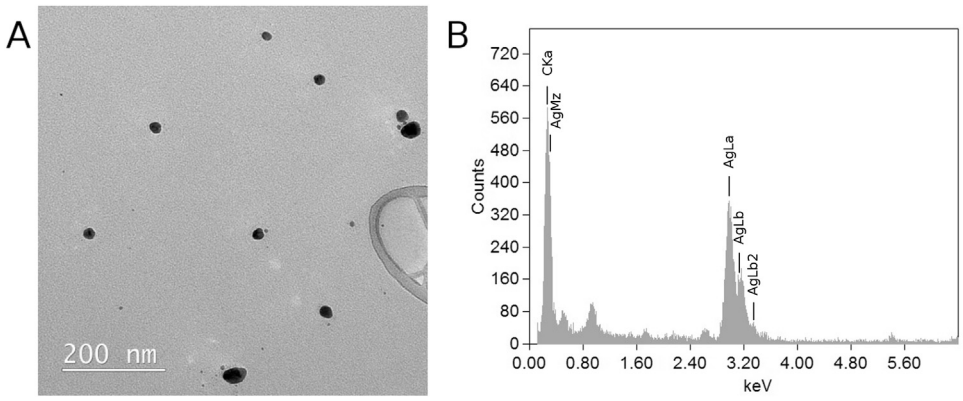

Fig. 2. Transmission electron microscopy image of P4C2- -induced silver nanoparticles. (**A**) Representative TEM image of peptide generated nanoparticles at magnification 50.000 x. Scale bar 200 nm (**B**) EDXS analysis of observed silver nanoparticles confirms silver composition of nanoparticles. C K line is from carbon coated carbon grid.

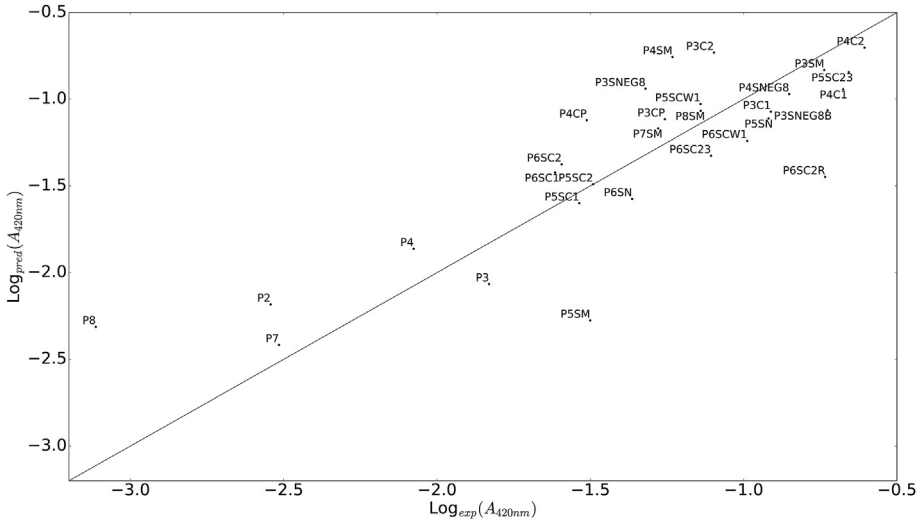

Fig. 3. Experimental AgNP formation propensity (absorbance values) versus model predictions based on the combination of sequence-defined predictors. R^2 for the proposed model equals 0.69. The model quality was evaluated using 10-fold cross validation (CV) yielding an average CV value of 0.27.

sequence, the number of alanine residues, maximal distance between basic residues, number of hydrophobic residues, average distance between hydrophobic residues, hydrophobic moment at 160° angle [26], and number of clusters consisting of a pair of hydrophobic residues. The first two listed descriptors are positively correlated with the capacity of peptides to make nanoparticles, while the rest are negatively correlated. Model-predicted and experimental A_{420nm} are in fair agreement with $R^2 = 0.69$ (see Fig. 3) . The model was validated with 10-fold cross validation (CV) yielding an average CV value of 0.27. While there have been numerous reports on peptide mediated reduction of silver ions [2–4,27,28], a detailed mechanistic analysis has yet to be put forward. There is some speculation which amino acid residues govern the observed phenomena, though a general consensus is still lacking. Our model shows that the presence of alanine residues negatively affects the AgNP formation in the investigated peptide set. Previous studies have shown that replacement of certain key residues with alanine leads to peptides unable of making silver nanoparticles [4,27]. The number of alanine residues in our set of peptides strongly influences the values of all descriptors aimed at describing hydrophobic properties of peptides. Results of the QSAR analysis hint that in our case glutamic acid and glutamine play a pivotal role in the reduction of silver ions. Side chain of glutamic acid contains a nucleophilic carboxylic group capable of coordinating silver ions, which in turn increases their local concentration and favorably affects the AgNP formation. Furthermore, it has been proposed that complexation of silver ions with carboxyl groups decreases the activation barrier for silver reduction [28,29]. Our results show glutamine may also contribute to the formation of AgNP. This was however observed only when two glutamine residues were separated from a lysine by a single amino acid residue. We speculate that this could be, similarly as with glutamic acid, a result of the coordination of silver ions by glutamine and lysine side chains. This is in accordance with the density function theory studies which predict a high silver ion binding affinity for both glutamine and lysine residues [30]. It is likely that the tyrosine residue at the C-terminus of the peptides is also involved in the silver reduction [29], but the effect of the Tyr residue on silver ion reduction cannot be evaluated in our set due to its presence in all designs.

3.3. Antibacterial activity

Since several peptides were shown to produce silver nanoparticles with antibacterial activities [31], we decided to investigate the antibacterial properties of peptide-induced AgNPs. P4C2

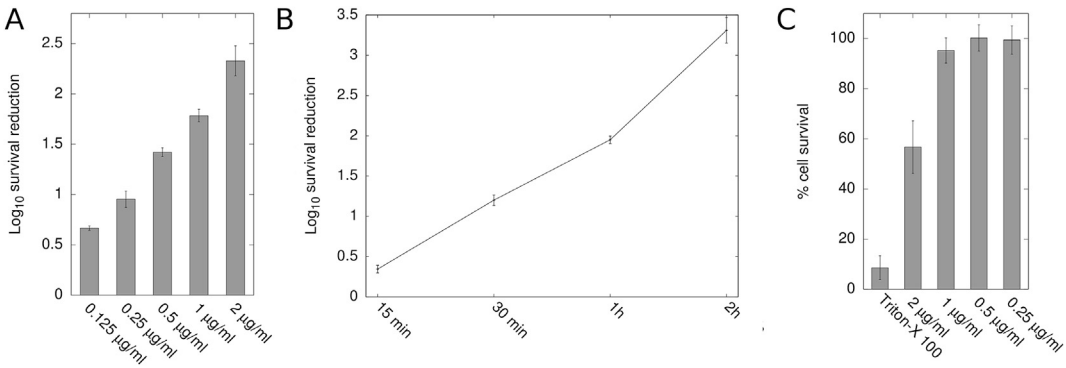

Fig. 4. Antimicrobial activity of P4C2 peptide-induced nanoparticles (**A**) Reduction of bacterial cell survival at different AgNP concentrations and (**B**) depending on the bacterial-AgNP contact time. Results are presented as log reduction of cell density (**C**) Cytotoxic effect of P4C2 generated nanoparticles on mammalian cells was evaluated against HEK293T cells. Results are presented as percentage of cell survival.

peptide, which produced the highest concentration of silver nanoparticles, was used to monitor the effect on bacterial growth. *E. coli* cells were incubated for 1 h with different concentrations of silver nanoparticles - 2 μg/ml, 1 μg/ml, 0.5 μg/ml, 0.25 μg/ml or 0.125 μg/ml in comparison to 5 mM sodium citrate as control (Fig. 4a). Duration of exposure of cells to silver nanoparticles was also evaluated. Cells were plated after a 15 min, 30 min, 1 h and 2 h incubation with AgNP. Two hours of silver nanoparticle exposure before plating, resulted in more than 99,9% of bacteria killed compared to the control (Fig. 4b) and even a short 15 min contact time of AgNP with bacteria exhibited bacterial killing. These results demonstrate the potential of this type of peptides as initiators of the AgNP formation, as they are able to mediate the formation of antibacterial AgNP in an environmentally friendly manner without harsh chemicals, at physiological pH and free from toxic byproducts. Furthermore, the peptides can be produced cost effectively on a large scale in recombinant form by the bacterial cells and used for quick and efficient AgNP formation.

Silver nanoparticles are steadily gaining importance in the medical field as antimicrobial agents. Their use is increasing rapidly; therefore it is important to consider the safety aspect of these nanosized materials. Several studies covered the subject extensively and explored adverse effects of nanoparticles on mammalian cells [32,33]. To assess the effect of nanoparticles on mammalian cells we exposed HEK293T cells to P4C2 generated silver nanoparticles at different concentrations overnight (Fig. 4c). Toxicity was observed for mammalian cells only at the highest used concentration, namely at 2 μg/ml. However at 1 μg/ml AgNP, a concentration at which an almost two log reduction in bacterial survival is observed in 2 h, 95% of the mammalian cells were viable after the overnight exposure. These results indicate that the silver nanoparticles described herein could be considered for further research for therapeutic applications, such as the design of antibacterial surfaces.

Acknowledgments

We thank Dr. Jelka Pohar for the help in performing experiments with mammalian cells. This work was financed by the program P4-0176 and projects L4-6812, J4-5528 financed by the Slovenian Research Agency (L4-6812 and J4-5528) and in part by the ERANET project Bioorigami (ERASYNBIO1-006) (to RJ) and an ICGEB project (CRP/SLO14-03) (to HG). Sabina Božič Abram is a PhD student at the Biomedicine program at the University of Ljubljana.

Transparency document

Transparency document related to this article can be found online at http://dx.doi.org/10.1016/j.bbrc.2016.03.042.

References

[1] M.B. Dickerson, K.H. Sandhage, R.R. Naik, Protein- and peptide-directed syntheses of inorganic materials, Chem. Rev. 108 (2008) 4935–4978.
[2] R.R. Naik, S.J. Stringer, G. Agarwal, S.E. Jones, M.O. Stone, Biomimetic synthesis and patterning of silver nanoparticles, Nat. Mater. 1 (2002) 169–172.
[3] E. Lee, D.-H. Kim, Y. Woo, H.-G. Hur, Y. Lim, Solution structure of peptide AG4 used to form silver nanoparticles, Biochem. Biophys. Res. Commun. 376 (2008) 595–598.
[4] K.-I. Sano, H. Sasaki, K. Shiba, Specificity and biomineralization activities of Ti-binding peptide-1 (TBP-1), Langmuir 21 (2005) 3090–3095.
[5] J.M. Fletcher, R.L. Harniman, F.R.H. Barnes, A.L. Boyle, A. Collins, J. Mantell, et al., Self-assembling cages from coiled-coil peptide modules, Sci. 340 (2013) 595–599.
[6] A. Lomander, W. Hwang, S. Zhang, Hierarchical self-assembly of a coiled-coil peptide into fractal structure, Nano Lett. 5 (2005) 1255–1260.
[7] S. Božič, T. Doles, H. Gradišar, R. Jerala, New designed protein assemblies, Curr. Opin. Chem. Biol. 17 (2013) 940–945.
[8] H. Gradišar, R. Jerala, De novo design of orthogonal peptide pairs forming parallel coiled-coil heterodimers, J. Pept. Sci. 17 (2011) 100–106.
[9] F. Thomas, A.L. Boyle, A.J. Burton, D.N. Woolfson, A set of de novo designed parallel heterodimeric coiled coils with quantified dissociation constants in the micromolar to sub-nanomolar regime, J. Am. Chem. Soc. 135 (2013) 5161–5166.
[10] C. Negron, A.E. Keating, A set of computationally designed orthogonal antiparallel homodimers that expands the synthetic coiled-coil toolkit, J. Am. Chem. Soc. 136 (2014) 16544–16556.
[11] C.W. Wood, M. Bruning, A.A. Ibarra, G.J. Bartlett, A.R. Thomson, R.B. Sessions, et al., CCBuilder: An interactive web-based tool for building, designing and assessing coiled-coil protein assemblies, Bioinformatics 30 (2014) 3029–3035.
[12] E. Cerasoli, B.K. Sharpe, D.N. Woolfson, ZiCo: a peptide designed to switch folded state upon binding zinc, J. Am. Chem. Soc. 127 (2005) 15008–15009.
[13] J.-B. Chang, Y.H. Kim, E. Thompson, Y.H. No, N.H. Kim, J. Arrieta, et al., The orientations of large aspect-ratio coiled-coil proteins attached to gold nanostructures, Small (2016) 1–8.
[14] M.-H. Yao, J. Yang, J.-T. Song, L. Zhang, B.-Y. Fang, D.-H. Zhao, et al., An engineered coiled-coil polypeptide assembled onto quantum dots for targeted cell imaging, Nanotechnol. 26 (2015) 495102.
[15] J.R. Morones, J.L. Elechiguerra, A. Camacho, K. Holt, J.B. Kouri, J.T. Ram, et al., The bactericidal effect of silver nanoparticles, Nanotechno. 16 (2005) 2346–2353.
[16] J.S.J.-H.J.S. Kim, E. Kuk, N. Yu, J.S.J.-H.J.S. Kim, S.J. Park, J. Lee, et al., Antimicrobial effects of silver nanoparticles, Nanomed. 3 (2007) 95–101.
[17] H. Lara, N. Ayala-Núñez, L. Ixtepan Turrent, C. Rodríguez Padilla, Bactericidal effect of silver nanoparticles against multidrug-resistant bacteria, World J. Microbiol. Biotechnol. 26 (2010) 615–621.
[18] J. Xie, J.Y. Lee, D.I.C. Wang, Y.P. Ting, Silver nanoplates: from biological to biomimetic synthesis, ACS Nano 1 (2007) 429–439.
[19] S. Si, T.K. Mandal, Tryptophan-based peptides to synthesize gold and silver nanoparticles: a mechanistic and kinetic study, Chem. - A Eur. J. 13 (2007) 3160–3168.
[20] U.O.S. Seker, H.V. Demir, Material binding peptides for nanotechnology, Mol. 16 (2011) 1426–1451.
[21] D. Paramelle, A. Sadovoy, S. Gorelik, P. Free, J. Hobley, D.G. Fernig, A rapid

method to estimate the concentration of citrate capped silver nanoparticles from UV–visible light spectra, Analyst 139 (2014) 4855–4861.
[22] D.A. Scudiero, R.H. Shoemaker, K.D. Paull, A. Monks, S. Tierney, T.H. Nofziger, et al., Evaluation of a soluble tetrazolium/formazan assay for cell growth and drug sensitivity in culture using human and other tumor cell lines, Cancer Res. 48 (1988) 4827–4833.
[23] S. Sánchez-Gómez, B. Japelj, R. Jerala, I. Moriyón, M.F. Alonso, J. Leiva, et al., Structural features governing the activity of lactoferricin-derived peptides that act in synergy with antibiotics against *Pseudomonas aeruginosa* in vitro and in vivo, Antimicrob. Agents Chemother. 55 (2011) 218–228.
[24] H. Gradišar, S. Božič, T. Doles, D. Vengust, I. Hafner-Bratkovič, A. Mertelj, et al., Design of a single-chain polypeptide tetrahedron assembled from coiled-coil segments, Nat. Chem. Biol. 9 (2013) 362–366.
[25] L.C. Gruen, Interaction of amino acids with silver(I) ions, Biochim. Biophys. Acta 386 (1975) 270–274.
[26] D. Eisenberg, R.M. Weiss, T.C. Terwilliger, The hydrophobic moment detects periodicity in protein hydrophobicity, Proc. Natl. Acad. Sci. U. S. A. 81 (1984) 140–144.
[27] C.J. Carter, C.J. Ackerson, D.L. Feldheim, Unusual reactivity of a silver mineralizing peptide, ACS Nano 4 (2010) 3883–3888.
[28] K.T. Nam, Y.J. Lee, E.M. Krauland, S.T. Kottmann, A.M. Belcher, Peptide-mediated reduction of silver ions on engineered biological scaffolds, ACS Nano 2 (2008) 1480–1486.
[29] S. Eckhardt, P.S. Brunetto, J. Gagnon, M. Priebe, B. Giese, K.M. Fromm, Nanobio silver: its interactions with peptides and bacteria, and its uses in medicine, Chem. Rev. 113 (2013) 4708–4754.
[30] J. Jover, R. Bosque, J. Sales, A comparison of the binding affinity of the common amino acids with different metal cations, Dalt. Trans. (2008) 6441.
[31] G. Ghodake, S.R. Lim, D.S. Lee, Casein hydrolytic peptides mediated green synthesis of antibacterial silver nanoparticles, Colloids Surf. B Biointerfaces 108 (2013) 147–151.
[32] A. Kunzmann, B. Andersson, T. Thurnherr, H. Krug, A. Scheynius, B. Fadeel, Toxicology of engineered nanomaterials: focus on biocompatibility, biodistribution and biodegradation, Biochim. Biophys. Acta - Gen. Subj. 1810 (2011) 361–373.
[33] A.M. Nyström, B. Fadeel, Safety assessment of nanomaterials: implications for nanomedicine, J. Control. Release 161 (2012) 403–408.